Biophysics and Physicobiology

Review Article (Invited)

Structural basis for Ca²⁺-dependent catalysis of a cutinase-like enzyme and its engineering: application to enzymatic PET depolymerization

Masayuki Oda

Graduate School of Life and Environmental Sciences, Kyoto Prefectural University, Kyoto 606-8522, Japan

A cutinase-like enzyme from *Saccharomonospora viridis* AHK190, Cut190, can depolymerize polyethylene terephthalate (PET). As high activity at approximately 70°C is required for PET depolymerization, structure-based protein engineering of Cut190 was carried out. Crystal structure information of the Cut190 mutants was used for protein engineering and for evaluating the molecular basis of activity and thermal stability. A variety of biophysical methods were employed to unveil the mechanisms underlying the unique features of Cut190, which included the regulation of its activity and thermal stability by Ca²⁺. Ca²⁺ association and dissociation can change the enzyme conformation to regulate catalytic activity. Weak metal-ion binding would be required for the naïve conformational change of Cut190, while maintaining its fluctuation, to "switch" the enzyme on and off. The activity of Cut190 is regulated by the weak Ca²⁺ binding to the specific site, Site 1, while thermal stability is mainly regulated by binding to another Site 2, where a disulfide bond could be introduced to increase the stability. Recent results on the structure-activity relationship of engineered Cut190 are reviewed, including the application for PET depolymerization by enzymes.

Key words: crystal structure, metal-ion binding, polyethylene terephthalate, thermal stability

Introduction

Cutinases belong to the lipase superfamily; these enzymes can hydrolyze complex plant biopolymers in the cutin (the cuticle layer of leaves) and various substrates, such as lipids, waxes, and synthetic esters [1]. Owing to the catalytic ability of ester bond hydrolysis, cutinases could be used as biocatalysts for the bioconversion of chemical compounds and degradation of polyethylene terephthalate (PET) into its two environmentally benign monomers: terephthalic acid and ethylene glycol [2]. PET has been extensively used worldwide, and waste PET has caused severe environmental problems. Chemical recycling of PET is important for sustainable development goals (SDGs). Enzymatic PET depolymerization is one of the most attractive methods due to its low energy consumption

Corresponding author: Masayuki Oda, Graduate School of Life and Environmental Sciences, Kyoto Prefectural University, 1-5 Hangi-cho, Shimogamo, Sakyo-ku, Kyoto 606-8522, Japan.
e-mail: oda@kpu.ac.jp

◄ *Significance* ►

Enzymatic depolymerization of polyethylene terephthalate (PET) followed by recycling is an attractive method for solving severe environmental problems worldwide. A cutinase-like enzyme, Cut190, is one such candidate enzymes, and engineered Cut190 mutants could catalyze substrates around the PET glass transition temperature. Crystal structure analysis of the Cut190 mutants in the absence or presence of Ca²⁺ and substrates revealed the presence of "open, closed, engaged, and ejecting" forms, which correspond to the respective conformations in the stages of catalysis. This review focuses on the Ca²⁺-regulated structure-activity relationship of Cut190 and its applications.

```
        50          60          70          80          90
     QDNPYE  RGPDPTEDSI  EAIRGPFSVA  TERVSSFASG  FGGGTIYYPR
        100         110         120         130         140
     ETDEGTFGAV  AVAPGFTASQ  GSMSWYGERV  ASQGFIVFTI  DTNTRLDQPG
        150         160         170         180         190
     QRGRQLLAAL  DYLVERSDRK  VRERLDPNRL  AVMGHSMGGG  GSLEATVMRP
        200         210         220         230         240
     SLKASIPLTP  WNLDKTWGQV  QVPTFIIGAE  LDTIASVRTH  AKPFYESLPS
        250         260         270         280         290
     SLPKAYMELD  GATHFAPNIP  NTTIAKYVIS  WLKRFVDEDT  RYSQFLCPNP
        300
     TDRAIEEYRS  TCPYKLN
```

Cut190*   S226P/R228S
Cut190**   S226P/R228S/K305del/L306del/N307del
Cut190*SS   Q138A/D250C-E296C/Q123H/N202H/S226P/R228S

Figure 1   The amino acid sequence of Cut190 and Cut190 mutants designated. The regions of helices and β-sheets are underlined in wavy and straight lines, respectively.

compared to conventional processes using supercritical fluids. High thermal stability is required for enzymatic PET depolymerization as the inner block of PET can only access the enzyme above the glass transition temperature (T_g) of approximately 70°C [3]. To our knowledge, at present, only four cutinases are categorized as PET hydrolases that significantly degrade the main body of PET into bis(hydroxyethyl)terephthalate (BHET), mono(hydroxyethyl) terephthalate, (MHET) or terephthalic acid [4].

A putative cutinase gene was cloned from the thermophile *Saccharomonospora viridis* AHK190, and its protein, Cut190, which is comprised of the residues Gln45-Asn307 (Fig. 1), was expressed in *Escherichia coli* [5]. The catalytic triad of Cut190, conserved in the lipase superfamily, was identified to include the residues Ser176, Asp222 and His254. One of the unique features of Cut190 is that its catalytic function and thermal stability are increased upon Ca^{2+} binding. The molecular mechanism of Cut190 regulation by Ca^{2+} binding has been analyzed using biophysical methods, including crystal structure and thermodynamic analyses. Using protein engineering based on structural information, such as "structure-based design", the thermal stability of Cut190 could be improved, in addition to the increase of the catalytic activity, making it possible to efficiently depolymerize PET above 70°C.

Cut190 mutants

In the course of amino acid substitution on Cut190 to increase its activity and stability, S226P and R228S mutations were first introduced [5]. The Pro residue corresponding to Ser226 in Cut190 is well conserved in homologous sequences of cutinases, and this mutation in Cut190 resulted in increased activity and thermal stability. Based on the crystal structure of Cut190S226P mutant described below, the mutation might break the hydrogen

bond of Ser226 with Thr221, affecting the activity and thermal stability. As Arg228 in Cut190 is considered to form a salt-bridge with acidic residues, which could influence the activity, a neutral amino acid substitution, such as R228S mutation, was introduced. The catalytic activity of S226P/R228S mutant was 1.5-fold higher than that of S226P mutant. Therefore, the mutant S226P/R228S designated as Cut190* was used as a template to introduce further mutations to increase its activity and thermal stability (Table 1) [6–8]. Upon the S176A mutation on Cut190*, no activity was observed even at a concentration 20-fold higher than that of Cut190*. Ser176 was determined to be the catalytic residue, as expected from the catalytic triad described above.

Because the crystal structures of Cut190 S226P and Cut190* mutants have been determined, they could be used as templates to generate Cut190 mutants with a "structure-based design". Mutation studies were carried out not only to increase activity and thermal stability, but also to determine the role of each residue. Using the crystal structures of Cut190 S226P in Ca^{2+}-bound and -unbound states, the model structures in complex with PET-like substrates were built, and the residues were selected to analyze their effects on catalytic activity and thermal stability [9]. In this strategy, the mutation sites were classified into three groups: (i) vicinity of the oxyanion hole, resulting in a decrease in the activation energy needed for catalysis, (ii) vicinity of the catalytic triad, and (iii) amino acids presumably interacting with the Ca^{2+}-bound form, but not with the Ca^{2+}-unbound form. For example, the F106A mutation in group (i) decreased the activity, while the F106Y mutation retained its activity, indicating that the aromatic residue at 106 is indispensable for hydrophobic interactions with the substrate. We found that mutation at Gln138 had strong effects; Q138A mutation contributed to increased enzymatic activity, while Q138L

Table 1   Thermal stabilities of Cut190 mutants

Metal (mM)	Ca^{2+} $T_{m,\ CD}$ (°C)	Ca^{2+} $T_{m,\ DSC}$ (°C)	Mn^{2+} $T_{m,\ CD}$ (°C)	Zn^{2+} $T_{m,\ CD}$ (°C)	Mg^{2+} $T_{m,\ CD}$ (°C)
Cut190*S176A					
0	53.6	54.4	53.6	53.6	53.6
0.25	59.6	—	62.7	61.1	56.2
2.5	64.4	63.5	64.2	60.5	n.d
25	67.8	67.2	66.1	n.d.	62.4
Cut190**S176A					
0	57.0	60.1	—	—	—
0.25	63.5	64.0	—	—	—
2.5	67.3	67.6	—	—	—
25	70.4	71.1	—	—	—
Cut190**					
0	60.3	65.3	—	—	—
0.25	69.1	69.2	—	—	—
2.5	72.1	72.7	—	—	—
25	75.7	76.4	—	—	—
Cut190*SS_S176A					
0	80.4	78.3	80.4	80.4	—
0.25	78.2	78.6	77.9	75.2	—
2.5	78.4	79.1	78.3	n.d.	—
25	79.8	80.8	78.4	n.d.	—
Cut190*SS					
0	82.1	82.8	82.1	82.1	—
0.25	82.5	82.9	82.1	79.5	—
2.5	83.3	83.4	82.7	n.d.	—
25	84.8	84.7	82.9	n.d.	—

$T_{m,\ CD}$ and $T_{m,\ DSC}$ are the values determined using CD and DSC, respectively. n.d.; Not determined due to the complexed transition. Data of Cut190**S176A and Cut190** analyzed using CD are first shown in this table, and other data are taken from previous papers [6–8].

mutation caused loss of activity, which could be a consequence of the additional space for the substrate generated by the mutation. The Q138A mutation resulted in decreased K_m and increased k_{cat} toward the aliphatic substrate, poly(butylene succinate-co-adipate) (PBSA), resulting in an approximately 4-fold increase in k_{cat}/K_m [10]. The activity was spectrophotometrically measured by monitoring the decrease in the turbidity of PBSA incubated with the enzyme at 37°C for 30 min. More precise analysis using HPLC showed that the main product of BHET catalyzed by Cut190* was MHET, possibly due to the low binding affinity of MHET [11].

Because Asn and Gln are prone to deamidation, leading to protein instability [12], surface Asn and Gln of Cut190* were mutated to other amino acids [10]. Among them, the most significant effect was observed in the N202H mutation; the T_m of Cut190*N202H was 6.5°C higher than that of Cut190*. Based on the crystal structures of Cut190* mutants described below, the salt bridge of His202 with Glu184 would contribute to the increased thermal stability. It should also be noted in Cut190*Q123H that the activity,

k_{cat}/K_m, was increased by approximately 1.5-fold with an increased T_m of 2.7°C. Both Gln123 and Asn202 are replaced with histidine in other homologous cutinases [10].

It is well known that disulfide bonds could contribute to increased protein stability [13]. However, increasing stability by mutations could result in significantly decreased activity in many cases, mainly because the naïve conformational change, including fluctuation, would be critical for activity [14]. In Cut190, Asp250 and Glu296 are located close to each other, and the Cys substitutions form a disulfide bond, which was confirmed by crystal structure analysis [6]. Upon mutation, T_m increased by 23°C [10]. Notably, the catalytic activity toward PBSA at 37°C upon the D250C/E296C mutation was almost unchanged. Altogether with other mutations that contribute to the increased activity and thermal stability, the mutant Q138A/D250C-E296C/Q123H/N202H/S226P/R228S, designated as Cut190*SS, was generated (Fig. 1), showing that T_m was 30°C higher than that of Cut190* (Table 1). Although the activity of Cut190*SS toward PBSA at 37°C was similar to that of Cut190*, the residual activity after incubating the

enzyme at 70°C was significantly enhanced [6,10]. The residual activities of Cut190* and Cut190*SS after incubation at 70°C for 2 h were approximately 10% and 95% relative to the activity without incubation, respectively [6]. These results strongly indicate that Cut190*SS is a promising candidate for PET degradation.

Crystal structure

In the series of structural analysis of Cut190 and its mutants, the crystal structures of the Cut190S226P mutant in the absence or presence of Ca^{2+} were first determined to 1.45 Å and 1.75 Å resolutions, respectively [PDB ID: 4WFI], [PDB ID: 4WFJ], [PDB ID: 4WFK] [15]. The enzyme was found to adopt a classical α/β hydrolase fold, which was comprised of a central twisted β-sheet of nine β-strands (β1-β9) and six α-helices (α2, α3, α5-α8), together with additional short helices, two α-helices (α1 and α4) and two 3_{10}-helices (η1 and η2) (Fig. 2A). Three catalytic residues, Ser176, Asp222, and His254, were located on the β5-α5, β7-α6, and β8-α7 loops, respectively. In the presence of Ca^{2+}, only one Ca^{2+} ion was observed in the β1-β2 loop. Upon Ca^{2+} binding, a large conformational change was observed in the three loops: β1-β2, β3-α2, and β4-α3 (Figs. 2B and 2C). Phe106 in the β3-α2 loop maintained the open conformation and formed an oxyanion hole. Ca^{2+} binding created an open space in the substrate-binding groove, which allowed the substrate to bind easily. Overall, Ca^{2+} binding could change the enzyme conformation from the "closed form" to the "open form".

To determine the complex structure with a substrate, an inactive mutant of Cut190*, Cut190*S176A, was crystallized [16]. Complexes with either monoethyl succinate or monoethyl adipate were successfully prepared by employing soaking methods, and the crystal structures were determined to 1.34 Å and 1.40 Å resolutions, respectively [PDB ID: 5ZRR], [PDB ID: 5ZRS]. Without substrates, the crystal structures complexed with metal-ions, only Ca^{2+} and a mixture of Ca^{2+} and Zn^{2+}, were also determined to 1.60 Å and 1.12 Å resolutions, respectively [PDB ID: 5ZNO], [PDB ID: 5ZRQ]. In contrast to the crystal structures of Cut190S226P [15], multiple metal-ion binding sites were observed. Together with the results of native mass spectrometry analysis for Ca^{2+} binding to Cut190*S176A in solution, three Ca^{2+} binding sites, Sites 1-3, were confirmed. At Site 1, Ca^{2+} was coordinated by the main chain carbonyls of Ser76, Ala78, and Phe81, and three water molecules, as observed in the structure of Cut190S226P [15]. At Site 2, Ca^{2+} was coordinated by the side chain carbonyls of Glu220, Asp250, and Glu296. At Site 3, Ca^{2+} was coordinated by the side chains of Asp204 and Thr206 and the main chain carbonyl of Thr206. In some crystal structures, Zn^{2+} ions were observed at Sites 2 and 3, possibly because Zn^{2+} was included in the crystallizing
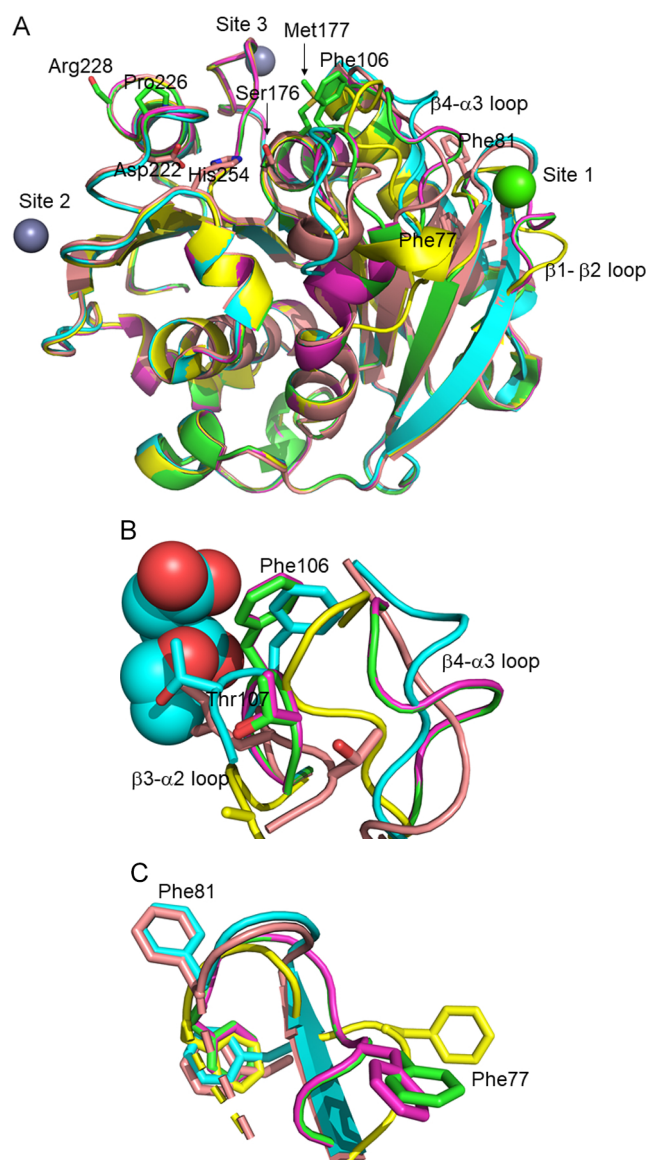

Figure 2 Crystal structures of Cut190 mutants. The structures of closed form (pink, PDB ID: 4WFI), open forms (without substrate; green, PDB ID: 5ZRQ, with substrate; purple, PDB ID: 5ZRS), engaged form (cyan; PDB ID: 5ZRR), and ejecting form (yellow, PDB ID: 7CEH) are superimposed. The figures were generated using the program PyMOL. (A) Overall structures. Spheres indicate bound metal ions. The side chains of Phe77, Phe81, Ser176, Asp222, His254 (PDB ID: 4WFI) and Phe106, Met177, Pro226, Arg228 (PDB ID: 5ZRQ) are also indicated as stick models. (B) Close-up view at β3-α2 and β4-α3 loops. The side chains of Phe106 and Thr107 are indicated as stick models and the substrate, monoethyl succinate, is indicated as a sphere model. (C) Close-up view at β1-β2 loop. The side chains of Phe77 and Phe81 are indicated as stick models.

solution and its binding affinity to the enzyme was higher than that of Ca^{2+}, as described below. In the absence of substrates, the crystal structure of Cut190*S176A with Ca^{2+} and Zn^{2+} adopted an "open form", similar to that of Cut190S226P. The crystal structure in complex with

monoethyl succinate demonstrated that the ester group of the substrate was located adjacent to Ala176, which was mutated from Ser176, the catalytic residue in the wild-type, and the carbonyl group of the ester was placed at the oxyanion hole contributed by the main chains of Phe106 and Met177 (Fig. 2B). Conformational changes were observed in the β3-α2 and β4-α3 loops (Fig. 2B). In the β3-α2 loop, Thr107 moved to the vicinity of the ester group and formed a hydrogen bond to stabilize the bound substrate. The results indicated that the structure corresponded to the pre-reaction state of the enzyme. The structure was different from either the "closed form" or the "open form", and was designated as the "engaged form". Notably, no metal-ions, neither Ca^{2+} or Zn^{2+}, were observed at Site 1, while Zn^{2+} ions were observed at Sites 2 and 3, indicating that substrate binding causes the release of Ca^{2+} at Site 1. The conformation of the β1-β2 loop in the engaged form was similar to that in the closed form, and the conformational changes in the β3-α2 and β4-α3 loops would be sufficient to accommodate and hydrolyze the substrate. In contrast, the crystal structure in complex with monoethyl adipate showed that the ester group of the substrate was located on the opposite side of the active site, and the oxygen atoms of the carboxyl group were located at the oxyanion hole and with His254 in a hydrogen bond, respectively. The results indicated that the structure corresponded to the post-reaction state of the enzyme. The structure was similar to the open form, and Ca^{2+} was observed to bind at Site 1.

In addition to the closed, open, and engaged forms, an "ejecting form" was observed in the crystal structure of Cut190**S176A, in which C-terminal 3 residues of Cut190*S176A were deleted (Fig. 1), in complex with Ca^{2+}, determined to a resolution of 1.09 Å [PDB ID: 7CEH] [17]. Ca^{2+} ions were observed at Sites 2 and 3, but not at Site 1. In the open form (Ca^{2+} at Site 1), Phe81 in the β1-β2 loop showed an inward conformation. In the closed and engaged forms (no Ca^{2+} at Site 1), Phe81 showed an outward conformation and Phe77 showed an inward conformation instead of Phe81 (Fig. 2C). The structure in ejecting form (no Ca^{2+} at Site 1) exhibited the inward conformation of Phe81. Because the ejecting form is similar to the closed form at the active site, substrate incompatible conformation, and like the open form at Site 1, the structure would be an intermediate during the turnover from the product release to re-activate for the next round of the reaction cycle.

The four observed structures are snapshot structures of Cut190 in solution, indicating the enzyme undergoes structural changes upon binding of Ca^{2+} and the substrate and the subsequent catalysis. This motion was supported by analyses using molecular dynamics (MD) simulations [16]. The closed and open forms were also observed in the crystal structures of Cut190**, Cut190*SS, and

Cut190*SS_S176A, determined to 1.60 Å, 1.20 Å, and 1.10 Å resolutions, respectively [PDB ID: 7CEF], [PDB ID: 7CTR], [PDB ID: 7CTS] [6,17]. In Cut190**, the asymmetric unit contained two molecules, and, surprisingly, one showed an open form, whereas the other showed a closed form. Zn^{2+} ions contained in the crystallization conditions were observed at Sites 2 and 3 in both molecules, while Ca^{2+} was only observed at Site 1 in the open form. The enzyme would fluctuate in solution, changing its form and possibly changing the population of the respective forms upon the association and dissociation of Ca^{2+}. The crystal structure may correspond to the most populated structure in solution. The supplementary movie shows the enzymatic reaction process via the obtained coarse snapshots (Supplementary Movie S1).

Metal-ion binding

As described above, the catalytic activity and thermal stability of Cut190 and its mutants increased upon Ca^{2+} binding. Analysis of the crystal structures strongly indicated that Ca^{2+} bound to multiple sites of Cut190 and induced a conformational change. In addition to the binding, Ca^{2+} dissociation from the enzyme could regulate the cycling of its catalytic function [16]. Moreover, other metal ions can bind to Cut190 and increase its activity and thermal stability. Metal-binding analysis using isothermal titration calorimetry (ITC) revealed endothermic heats for Zn^{2+}, Mn^{2+}, and Mg^{2+} binding (Fig. 3). The binding affinities of Zn^{2+} and Mn^{2+} were approximately one order of magnitude higher than that of Mg^{2+} [7]. In contrast, little heat upon Ca^{2+} binding was observed (Fig. 3D), possibly due to the weak binding affinity with a small binding enthalpy change. Notably, the binding stoichiometry of Zn^{2+} was approximately 3, while that of Mn^{2+} and Mg^{2+} was approximately 1. As determined by the crystal structure and native mass spectrometry analyses, three binding sites, Sites 1–3, existed, which was in good agreement with the stoichiometry of Zn^{2+}. 3D Reference Interaction Site Model (RISM) calculations also supported the multivalent metal-ion binding sites and further indicated the order of binding affinity at each site: Site 2>Site 3>Site 1 [16]. The occupancy values in RISM calculations also indicated that the binding affinities of Mn^{2+} and Zn^{2+} were higher than that of Ca^{2+} [7]. Altogether, Mn^{2+} and Mg^{2+} might be able to bind to Site 2 with high affinity, enabling the heat observable in ITC, and bind to other sites with low affinity. The catalytic activity of Cut190 would largely depend on the metal-ion binding affinity, especially at Site 1. The activities of Cut190* toward PBSA in the presence of 0.25 mM Mn^{2+} and 2.5 mM Mg^{2+} were approximately 90% and 40% of that in the presence of 2.5 mM Ca^{2+}, respectively, whereas that in the presence of Zn^{2+} was markedly lower [7]. The results indicated that the order
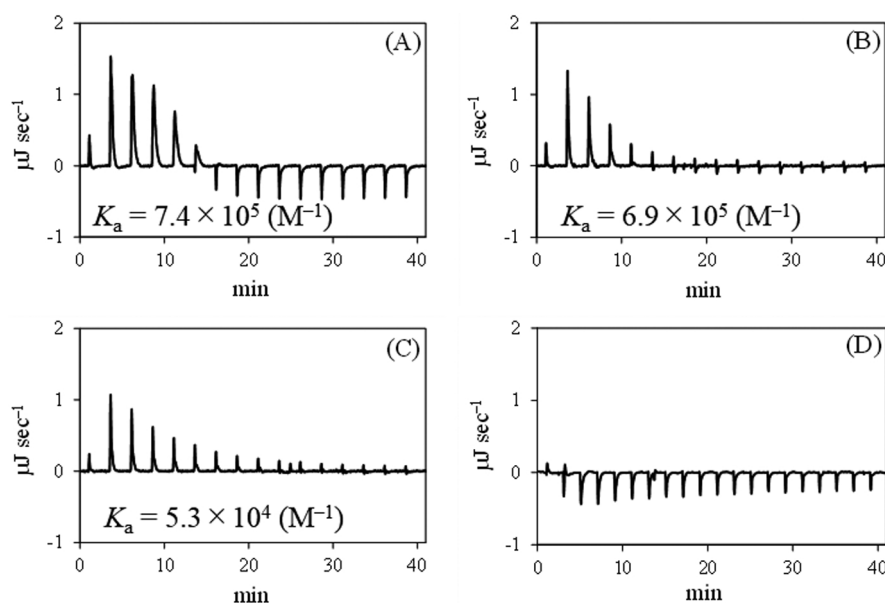
Figure 3 ITC profiles of metal-ion binding to Cut190*S176A at 25°C. A solution of $ZnCl_2$ (A), $MnCl_2$ (B), $MgCl_2$ (C), and $CaCl_2$ (D) was injected into Cut190*S176A on iTC200 calorimeter. The K_a values are also indicated.

of binding affinity at Site 1 was $Ca^{2+}<Mg^{2+}<Mn^{2+}<Zn^{2+}$.

ITC experiments revealed no binding heats of metal ions, even Zn^{2+}, for Cut190*SS and Cut190*SS_S176A, in which disulfide bonds were introduced at residues 250 and 296, close to Site 2 [6]. Upon mutation, not only Site 2, but also other metal-binding sites would be perturbed for metal binding. The crystal structures of Cut190*SS and Cut190*SS_S176A showed no metal ions at Sites 2 and 3. Similar to Cut190*, the catalytic activity of Cut190*SS was observed in the presence of metal ions, indicating that the weak metal-ion binding at Site 1 was preserved. This is also supported by the crystal structure of Cut190*SS_S176A (open form), in which Ca^{2+} binding was only observed at Site 1. The activity gradually increased, depending on the Ca^{2+} concentration, and was the highest under 5 mM Ca^{2+}, which was markedly higher than that in the presence of Zn^{2+} or Mn^{2+} [6].

The importance of weak metal-ion binding for enzyme function was also reported in the case of ribonuclease H [18], and the Mg^{2+} binding sites on ribonuclease H remain controversial [19]. Similar to the case of Ca^{2+} binding to Cut190, ribonuclease H of human immunodeficiency virus binds to Mg^{2+} weakly, much weaker than Mn^{2+} and Zn^{2+}. Zn^{2+} at low concentration catalyzes the activity of ribonuclease H similar to Mg^{2+}, while Zn^{2+} at high concentration inhibits the activity [20]. The weak binders would be advantageous to regulate enzyme activity; meal ions could associate and dissociate from enzyme to "switch" the activity on and off. Further, the enzyme conformation could gradually change while maintaining

proper fluctuation. More precise and innovative analyses, such as single-molecule analysis, will provide more details on the enzyme structure-activity relationship and the role of weak metal-ion binding.

Folding thermodynamics

Thermal stability was determined using circular dichroism (CD) and differential scanning calorimetry (DSC) experiments, which detect changes in the secondary structure and heat capacity upon the transition, respectively. Although the thermal transition of Cut190 and its mutants was irreversible, the folding thermodynamics were determined using a fitting procedure, assuming a two-state transition between folded and unfolded states. The thermal stability of Cut190*S176A increased as Ca^{2+} concentration increased (Table 1), mainly due to the more favorable enthalpy change [8]. The MD simulations of both the Ca^{2+}-unbound and Ca^{2+}-bound structures supported the notion that Ca^{2+} binding to Cut190*S176A increased the thermal stability by increasing enthalpy change and decreasing entropy change, which might be due to the increase in intramolecular interactions and the decrease in structural flexibility. In the presence of other metal ions, Zn^{2+}, Mn^{2+}, and Mg^{2+}, the thermal stability of Cut190*S176A increased in the concentration range lower than Ca^{2+} (Table 1). The respective thermal stabilities in the presence of 0.25 mM metal ions were ordered as $Mg^{2+}<Ca^{2+}<Mn^{2+}<Zn^{2+}$, while those in the presence of 25 mM metals were ordered as $Mg^{2+}<Mn^{2+}<Ca^{2+}$. In the presence of 25 mM Zn^{2+},

Cut190*S176A became aggregated. Taken together with the results of the metal-binding affinity assay described above, a strong binder would increase the intramolecular interactions at low concentrations, resulting in increased thermal stability, and would increase them too much at high concentrations, resulting in aggregation.

Upon deletion of the C-terminal 3 residues of Cut190*S176A, the thermal stability increased, mainly because of the favorable entropy change [17]. One possible explanation for this is the decreased fluctuation in the unfolded state. Another explanation is the multiple states that exist in the folded state. This might align with the observation that the asymmetric unit in the crystal structure of Cut190** contained two molecules, one in an open form and the other in a closed form, as described above. The thermal stability of Cut190**S176A was higher than that of Cut190**, similar to the case of Cut190*SS_S176A and Cut190*SS [6]. This would be mainly due to the salt bridge between Ser176 and His254 in the catalytic triad. Among the mutants analyzed so far, Cut190*SS, whose T_m in the absence of metal ion was 82°C and increased up to 85°C in the presence of 25 mM Ca^{2+}, was the most stable. This Ca^{2+}-dependent increase in thermal stability supported the notion that Ca^{2+} could bind to Cut190*SS and regulate its function, despite no metal-ion binding being observed in ITC. 3D-RISM calculations indicated that the binding affinity at Site 1 was almost unchanged, while those at Sites 2 and 3 were reduced due to the mutations directly made to Site 2 (D250C and E296C) and the mutation of a residue near Site 3 (N202H). The disulfide-bond introduction between the residues at 250 and 296 would largely contribute to increased thermal stability, possibly similar to the effects of metal-ion binding at Site 2 of the enzyme without the disulfide bond. The introduction of disulfide bonds to the corresponding site was also reported in mutants of the related enzyme, leaf-branch compost cutinase (LCC) [21].

Application

PET depolymerization by enzymes and their subsequent recycling have been investigated worldwide for SDGs and severe environmental problems. Tournier *et al.* reported that LCC mutants could be used to recycle all types of PET waste [21]. LCC was first cloned from a fosmid library of a leaf-branch compost metagenome by Kanaya's group [22], and the crystal structure was subsequently determined [23]. The T_m value of LCC wild-type was 85°C, and that of the mutant with the disulfide-bond introduction increased to 94°C. The overall crystal structures of LCC mutants were similar to those of Cut190 mutants [PDB ID: 6THT], [PDB ID: 6THS] (Fig. 4). In the β1-β2 loop region at Site 1, the enzymes related to LCC were found to be one residue longer than Cut190. The insertion of Ser into
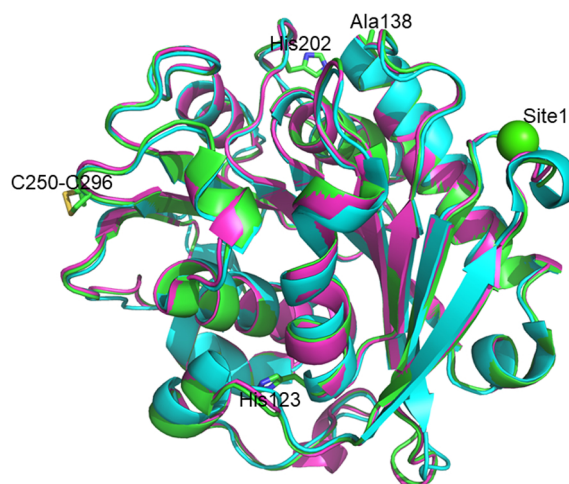

Figure 4   Crystal structures of Cut190*SS_S176A (green, PDB ID: 7CTS), LCC mutant Y127G/S165A/D238C/F243I/S283C (cyan, PDB ID: 6THT), and Cut190** (purple, PDB ID: 7CEF). A sphere indicates Ca^{2+} bound to Cut190*SS_S176A. The side chains of His123, Ala138, His202 and the disulfide bond of Cut190*SS_S176A are indicated as stick models. The figure was generated using the program PyMOL.

Cut190* at this site resulted in expressing the activity even in the absence of Ca^{2+} [10]. Tournier *et al.* showed that LCC mutant Y127G/D238C/F243W/S283C ultimately achieved a T_m of 98°C and 90% PET depolymerization into monomers over a 10 h reaction [21]. Because the corresponding residues in Cut190* are Q138A/D250C/F255/E296C, the mutations of Q138G and F255W in Cut190*SS might increase the activity and thermal stability. They also showed that the reaction temperature could be increased to 72°C to maximize kinetic turnover, because PET was largely recrystallized above 75°C. The low crystallinity of PET is also critical for efficient PET depolymerization. Miyamoto's group reported that the addition of anionic surfactants was effective at inducing efficient PET depolymerization by a cationic PET hydrolase identified from *Ideonella sakaiensis* [24,25]. The reaction was also effective under high pressure [11].

The economics of enzymatic processing is of the utmost importance when considering the industrial applications of PET recycling. Although engineered proteins have been considered inappropriate as pharmaceuticals, mainly because of costs, numerous protein pharmaceuticals, such as antibody drugs, have been used recently. Challenging the goal of PET recycling using enzymes is important and contributes to basic science in a wide range of fields, such as protein chemistry and polymer chemistry.

Conflicts of Interest

The authors declare that they have no conflicts of interest with the contents of this article.

Author Contributions

MO wrote this review.

References

[1] Chen, S., Su, L., Chen, J. & Wu, J. Cutinase: characteristics, preparation, and application. *Biotechnol. Adv.* **31**, 1754–1767 (2013). DOI: 10.1016/j.biotechadv.2013.09.005

[2] Kawai, F., Kawabata, T. & Oda, M. Current knowledge on enzymatic PET degradation and its possible application to waste stream management and other fields. *Appl. Microbiol. Biotech.* **103**, 4253–4268 (2019). DOI: 10.1007/s00253-019-09717-y

[3] Zimmermann, W. & Billig, S. Enzymes for the biofunctionalization of poly(ethylene terephthalate). *Adv. Biochem. Eng. Biotechnol.* **125**, 97–120 (2011). DOI: 10.1007/10_2010_87

[4] Kawai, F., Kawabata, T. & Oda, M. Current state and perspectives related to the PET hydrolases available for biorecycling. *ACS Sustainable Chem. Eng.* **8**, 8894–8908 (2020). DOI: 10.1021/acssuschemeng.0c01638

[5] Kawai, F., Oda, M., Tamashiro, T., Waku, T., Tanaka, N., Yamamoto, M., *et al.* A novel Ca^{2+}-activated, thermo-stabilized polyesterase capable of hydrolyzing polyethylene terephthalate from *Saccharomonospora viridis* AHK190. *Appl. Microbiol. Biotechnol.* **98**, 10053–10064 (2014). DOI: 10.1007/s00253-014-5860-y

[6] Emori, M., Numoto, N., Senga, A., Bekker, G.-J., Kamiya, N., Kobayashi, Y., *et al.* Structural basis of mutants of PET-degrading enzyme from *Saccharomonospora viridis* AHK190 with high activity and thermal stability. *Proteins* **89**, 502–511 (2021). DOI: 10.1002/prot.26034

[7] Senga, A., Hantani, Y., Bekker, G.-J., Kamiya, N., Kimura, Y., Kawai, F., *et al.* Metal binding to cutinase-like enzyme from *Saccharomonospora viridis* AHK190 and its effects on enzyme activity and stability. *J. Biochem.* **166**, 149–156 (2019). DOI: 10.1093/jb/mvz020

[8] Inaba, S., Kamiya, N., Bekker, G.-J., Kawai, F. & Oda, M. Folding thermodynamics of PET-hydrolyzing enzyme Cut190 depending on Ca^{2+} concentration. *J. Therm. Anal. Calorim.* **135**, 2655–2663 (2019). DOI: 10.1007/s10973-018-7447-9

[9] Kawabata, T., Oda, M. & Kawai, F. Mutational analysis of cutinase-like enzyme, Cut190, based on the 3D docking structure with model compounds of polyethylene terephthalate. *J. Biosci. Bioeng.* **124**, 28–35 (2017). DOI: 10.1016/j.jbiosc.2017.02.007

[10] Oda, M., Yamagami, Y., Inaba, S., Oida, T., Yamamoto, M., Kitajima, S., *et al.* Enzymatic hydrolysis of PET: Functional roles of three Ca^{2+} ions bound to a cutinase-like enzyme, Cut190*, and its engineering for improved activity. *Appl. Microbiol. Biotechnol.* **102**, 10067–10077 (2018). DOI: 10.1007/s00253-018-9374-x

[11] Hantani, Y., Imamura, H., Yamamoto, T., Senga, A., Yamagami, Y., Kato, M., *et al.* Functional characterizations of polyethylene terephthalate-degrading cutinase-like enzyme Cut190 mutants using bis(2-hydroxyethyl) terephthalate as the model substrate. *AIMS Biophysics* **5**, 290–302 (2018). DOI: 10.3934/biophy.2018.4.290

[12] Wright, H. T. Nonenzymatic deamidation of asparaginyl and glutaminyl residues in proteins. *Crit. Rev. Biochem. Mol. Biol.* **26**, 1–52 (1991). DOI: 10.3109/10409239109081719

[13] Yutani, K., Ogasahara, K. & Sugino, Y. Effect of amino acid substitutions on conformational stability of a protein. *Adv. Biophys.* **20**, 13–29 (1985). DOI: 10.1016/0065-227x(85)90028-0

[14] Oda, M., Furukawa, K., Ogata, K., Sarai, A. & Nakamura, H. Thermodynamics of specific and non-specific DNA binding by the c-Myb DNA-binding domain. *J. Mol. Biol.* **276**, 571–590 (1998). DOI: 10.1006/jmbi.1997.1564

[15] Miyakawa, T., Mizushima, H., Ohtsuka, J., Oda, M., Kawai, F. & Tanokura, M. Structural basis for the Ca^{2+}-enhanced thermostability and activity of PET-degrading cutinase from *Saccharomonospora viridis* AHK190. *Appl. Microbiol. Biotechnol.* **99**, 4297–4307 (2015). DOI: 10.1007/s00253-014-6272-8

[16] Numoto, N., Kamiya, N., Bekker, G.-J., Yamagami, Y., Inaba, S., Ishii, K., *et al.* Structural dynamics of PET-degrading cutinase-like enzyme from *Saccharomonospora viridis* AHK190 in substrate-bound states elucidates Ca^{2+} driven catalytic cycle. *Biochemistry* **57**, 5289–5300 (2018). DOI: 10.1021/acs.biochem.8b00624

[17] Senga, A., Numoto, N., Yamashita, M., Iida, A., Ito, N., Kawai, F., *et al.* Multiple structural states of Ca^{2+} regulated PET hydrolase, Cut190, and its correlation with activity and stability. *J. Biochem.* **169**, 207–213 (2021). DOI: 10.1093/jb/mvaa102

[18] Oda, M., Xi, Z., Inaba, S., Slack, R. L. & Ishima, R. Binding thermodynamics of metal ions to HIV-1 ribonuclease H domain. *J. Therm. Anal. Calorim.* **135**, 2647–2653 (2019). DOI: 10.1007/s10973-018-7445-y

[19] Ho, M.-H., De Vivo, M., Dal Peraro, M. & Klein, M. L. Understanding the effect of magnesium ion concentration on the catalytic activity of ribonuclease H through computation: does a third metal binding site modulate endonuclease catalysis? *J. Am. Chem. Soc.* **132**, 13702–13712 (2010). DOI: 10.1021/ja102933y

[20] Fenstermacher, K. J. & DeStefano, J. J. Mechanism of HIV reverse transcriptase inhibition by zinc: formation of a highly stable enzyme-(primer-template) complex with profoundly diminished catalytic activity. *J. Biol. Chem.* **286**, 40433–40442 (2011) DOI: 10.1074/jbc.M111.289850

[21] Tournier, V., Topham, C. M., Gilles, A., David, B., Folgoas, C., Moya-Leclair, E., *et al.* An engineered PET depolymerase to break down and recycle plastic bottles. *Nature* **580**, 216–219 (2020). DOI: 10.1038/s41586-020-2149-4

[22] Sulaiman, S., Yamato, S., Kanaya, E., Kim, J. J., Koga, Y., Takano, K., *et al.* Isolation of a novel cutinase homolog with polyethylene terephthalate-degrading activity from leaf-branch compost by using a metagenomic approach. *Appl. Environ. Microbiol.* **78**, 1556–1562 (2012). DOI: 10.1128/AEM.06725-11

[23] Sulaiman, S., You, D. J., Kanaya, E., Koga, Y. & Kanaya, S. Crystal structure and thermodynamic and kinetic stability of metagenome-derived LC-cutinase. *Biochemistry* **53**, 1858–1169 (2014). DOI: 10.1021/bi401561p

[24] Yoshida, S., Hiraga, K., Takehana, T., Taniguchi, I., Yamaji, H., Maeda, Y., *et al.* A bacterium that degrades and assimilates poly(ethylene terephthalate). *Science* **351**, 1196–1199 (2016). DOI: 10.1126/science.aad6359

[25] Furukawa, M., Kawakami, N., Oda, K. & Miyamoto, K. Acceleration of enzymatic degradation of poly(ethylene terephthalate) by surface coating with anionic surfactants. *ChemSusChem* **11**, 4018–4025 (2018). DOI: 10.1002/cssc.201802096

(*Edited by Daisuke Kohda*)